

Crystallization of HWCVD amorphous silicon thin films at elevated temperatures

Theo F.G. Muller^{a,*}, Dirk Knoesen^a, Chris Arendse^a, Ryno Swanepoel^a,
Sylvain Halindintwali^a, Chris Theron^b

^a Department of Physics, University of the Western Cape, Private Bag X17, Bellville 7535, South Africa

^b iThemba Labs, P. O. Box 722, Somerset West 7129, South Africa

Available online 8 November 2005

Abstract

Hot-wire chemical vapour deposition (HWCVD) has been used to prepare both hydrogenated amorphous silicon (a-Si:H) and nano/microcrystalline thin layers as intrinsic material at different deposition conditions, in order to establish optimum conditions where the hydrogen content would be minimal and the films would still exhibit good optical properties. Experimental data shows that by varying deposition conditions the transition to the nano/microcrystalline phase can be achieved. Transitional films in the regime tending towards the crystalline phase showed no infrared-active hydrogen. XRD analysis failed to show any discernible crystalline peaks, while Raman spectroscopy as a tool is more promising for the identification of films in changeover to the nano/microcrystalline state.

© 2005 Elsevier B.V. All rights reserved.

Keywords: Crystallization; Silicon; Phase transitions; Structural properties

1. Introduction

Currently, the deposition of nano- and microcrystalline silicon (nc-Si:H and μ c-Si:H) thin films by hot-wire chemical vapour deposition (HWCVD) is becoming more common [1,2], while hydrogenated amorphous silicon (a-Si:H) deposited in HWCVD reactors has been extensively studied. HWCVD offers many advantages. It has relatively high deposition rates compared to the established Plasma-Enhanced Chemical Vapour Deposition (PECVD) technique [3] and it suffers no ion damage during deposition. The films can be deposited at relatively low substrate temperatures for utilization of cheap, flexible substrates and still retain reasonable device-quality properties [4]. Another added benefit is that films deposited by HWCVD have shown good resistance to the Staebler–Wronski effect [5], a condition whereby film properties degrade under prolonged exposure to light [6].

In laboratories around the world, HW-films that exhibit crystalline properties were obtained by changing various deposition parameters, e.g. varying the chamber pressure during deposition [7] and varying the H₂/SiH₄ ratio [8]. The dilution of silane with hydrogen leads to reduced deposition rates [8], however these rates are still favourable to the deposition rates of other methods.

In this study, a set of intrinsic samples was grown using the HWCVD method in order to examine the role of H₂ dilution in phase transitions and its effect on the deposition rate. The optical and structural properties, as well as the incorporation of hydrogen into the films will be discussed for films deposited at different substrate temperatures.

2. Experimental details

Thin silicon films of thickness ranging between 280 and 860 nm were deposited onto Corning 7059 glass and $\langle 100 \rangle$ c-Si substrates in a single-chamber HWCVD reactor. Dissociation of the reactant gases SiH₄ and H₂ occurred over a tantalum (Ta) filament that consisted of seven parallel

* Corresponding author. Tel.: +27 219592328; fax: +27 219591269.

E-mail address: tmuller@uwc.ac.za (T.F.G. Muller).

Table 1
Deposition conditions for different HWCVD films

	Film A	Film B	Film C	Film D
T_{fil} (°C)	1600	1600	1600	1600
T_{sub} (°C)	462	706	417	417
$d_{\text{s-f}}$ (cm)	1.8	1.8	1.8	1.8
P (pa)	8	8	2	2
$\Phi_{(\text{SiH}_4)}$ (sccm)	60	60	7.5	3.3
$\Phi_{(\text{H}_2)}$ (sccm)	–	–	30	30

Film C (80%) and film D (90%) were deposited under hydrogen dilution conditions.

wires maintained at 1600 °C. The substrate to filament distance ($d_{\text{s-f}}$) was fixed at 1.8 cm and different substrate temperatures, pressures and gas flow rates were used as shown in Table 1. Film A was deposited as a standard under conditions that literature predicted would yield good amorphous material.

The refractive index, absorption coefficient, and energy band gap were deduced from Optical Transmission Spectroscopy following Swanepoel [9]. The hydrogen content C_{H} and microstructure factor $R^* = ((I_{2090}) / (I_{2000} + I_{2090}))$, where I_{2000} and I_{2090} refer to the integrated intensities at the respective wavenumbers, were obtained from Fourier Transmission Infrared Spectroscopy (FTIR) measurements, using proportionality constants proposed by Ouwens [10]. The total hydrogen content was also determined with the Elastic Recoil Detection (ERD) technique using a $^4\text{He}^+$ beam at 3 MeV. The structure of the films was investigated with XRD analysis using the Cu K_{α} wavelength of 0.1542 nm. The amount of disorder (bond angle variation ϑ_{b}) and crystalline fraction X_{c} were calculated from Raman spectroscopy, using a configuration similar to that of Berntsen [11]. The crystalline fraction was determined from $X_{\text{c}} = ((I_{\text{c}} + I_{\text{gb}}) / (I_{\text{c}} + I_{\text{gb}} + I_{\text{a}}))$ where I_{c} , I_{gb} and I_{a} are the integrated intensities of the crystalline, intermediate peaks of the amorphous to crystalline phase, and the amorphous phases, respectively [12].

3. Results and discussion

3.1. Optical properties and hydrogen incorporation

The absorption curves in Fig. 1 show good absorption of greater than 10^4 cm^{-1} for all the films. The reference sample at 462 °C (Film A) shows similar absorption to the film of 90% hydrogen dilution (Film D); for $\alpha_{2\text{eV}}$, the film deposited at 706 °C (Film B) shows the most absorption. The extreme thermal conditions and long heating time for the substrate should disqualify Film B for utilization as intrinsic material. Rutherford backscattering spectrometry confirms that no impurities, like iron that could possibly have originated from the chamber walls, are present in this film. Absorption for Film C (80% dilution) is the least; its absorption and other features distinguish it from the other films. Band gap values of these films are consistent with

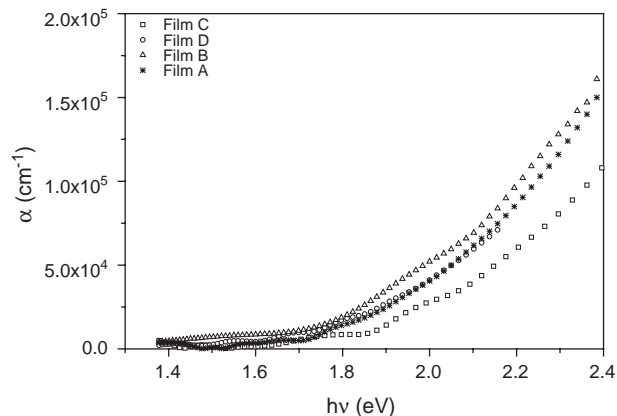


Fig. 1. Absorption curves for Si thin films as function of energy.

those of hydrogenated amorphous silicon thin films (see Table 2); the reduced value for Film D is probably an indication that this film is undergoing a phase transition whereby small crystallites are included in the bulk of the amorphous layer. XRD analysis in the next section will further examine this aspect. The refractive index, $n_{2\text{eV}}$ is similar for all films except Film C, implying a reduced optical density for this film. The reduction in deposition rates for the films under hydrogen dilution is as expected, but the deposition rate still compares favourably with those of PECVD.

Apart from the reference sample (Film A), none of the films had any bonded hydrogen that could be detected with FTIR. This does not augur well for device properties, as the bonded hydrogen is required to passivate dangling bond defects [13]. One critical aspect of Film A is that the hydrogen is only bonded in the 2000 cm^{-1} mode and none in the 2090 cm^{-1} mode. This yields a structure factor of much less than 0.1, indicative of device-quality amorphous material. Due to its high processing temperature, Film B was not expected to contain much bonded hydrogen, while Films C and D were expected to contain at least a fraction of a percent of bonded hydrogen for passivation purposes. Normally, hydrogen dilution leads to a reduction in bonded hydrogen content [8], but a relatively high processing temperature (417 °C in this case) probably enhanced hydrogen evolution from the bonds. ERD gives a total hydrogen concentration in the film and not just the bonded hydrogen. The results (not shown) for the hydrogen dilution films (Films C and D) reveals that Film C only has a fraction of an atomic percent hydrogen (0.6 at.%) while Film D actually contains ~ 4 at.% hydrogen in the bulk of the film.

Table 2
Optical properties of films deposited by HWCVD

	d (nm)	r_{d} (nm/s)	E_{g} (eV)	$n_{2\text{eV}}$	FTIR C_{H} (at.%)
Film A	530	1.77	1.74	4.22	1.6
Film B	285	2.40	1.72	4.26	–
Film C	560	0.46	1.73	3.82	–
Film D	858	0.45	1.58	4.19	–

The only inference that can be made is that the hydrogen must exist in the form of molecular H_2 trapped in voids. Nuclear Magnetic resonance (NMR) studies of both PECVD and HWCVD a-Si:H films [14] have focussed on the detection of molecular hydrogen and confirmed the existence thereof. These studies identified two local environments, one where the molecular hydrogen contribute to the relaxation of the network of atoms and the other instance where it does not [15]. In these studies, the quantities of molecular hydrogen in the hot-wire films were quite small; but never to an extent such as for our films. Positron annihilation defect studies of some films manufactured in our reactor chamber are currently being undertaken to quantify the void fraction.

A proposed mechanism for these films is that radiative heat transfers from the filament to the substrate due to the effective large filament surface area. This adds to the total effect of hydrogen dilution on hydrogen incorporation. During growth, large amounts of atomic hydrogen are present in the chamber to bond to the Si dangling bonds. The hydrogen atoms either combine with other hydrogen atoms, to form H_2 gas that get trapped in the voids, or thermally break Si–H bonds. The hydrogen atoms then leave the bonding sites immediately after occupying the bonding sites and get trapped with other hydrogen atoms to form H_2 in the voids that are created. To ensure hydrogen passivation of the dangling bonds and to prevent incorporation of an excess amount of H_2 , lower processing substrate temperatures will be used in the reactor chamber in future.

3.2. Structural properties

Film A was expected to be amorphous and XRD confirmed its amorphous nature. Extreme thermal conditions for Film B raised the expectation that crystallization might have occurred, but its relatively large band gap value argued against this. Its XRD spectrum on glass actually did not show any discernable peak. The other two films also did not show any clear and high intensity peaks corresponding to any crystallographic orientation (Fig. 2). The assumption

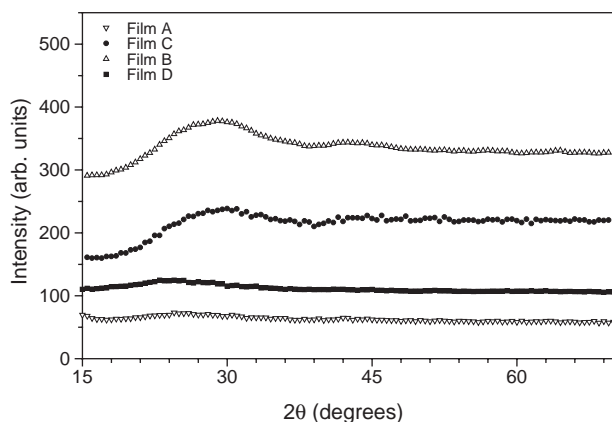


Fig. 2. Stacked XRD spectra as a function of diffracting angle.

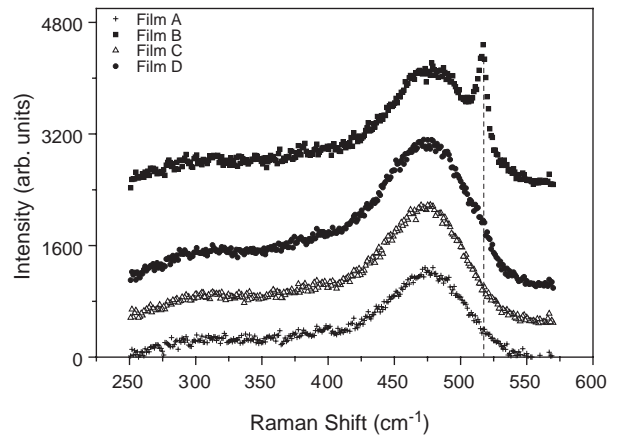


Fig. 3. Raman spectra for the HWCVD films.

would thus be that all these films are amorphous. To test the validity of the assumption Raman scattering experiments were carried out, with unexpected results. The highly visible 520 cm^{-1} peak for Film B clearly indicates the crystalline nature of the film, showing a crystalline volume fraction of 13.6%. The other three films should be amorphous due to the absence of peaks at 520 cm^{-1} (Fig. 3). Careful scrutiny of the spectrum of Film D revealed a small hump on the high-energy side; this shoulder actually gives a crystalline fraction of 4.7%—suggestive of a film that underwent a nanocrystalline phase transition. Films A and C, although amorphous, have bond angle variations (ϑ_b) of 7.1° and $\leq 6.6^\circ$, respectively; excellently ordered films. This is equivalent to Raman TO half widths of $< 32\text{ cm}^{-1}$. Beeman et al. [16] considered ϑ_b values of $< 6.6^\circ$ to be that of films in the crystalline transition regime. Previous attempts to detect very small crystallites in bulk a-Si:H thin films by XRD were complicated [17]. It was found that the XRD FWHM of the proto-crystallites became comparable with the width of the amorphous signal, making the detection thereof too difficult. On the other hand, Raman spectroscopy is shown here to be especially helpful in qualitatively detecting very small volume fractions of small crystallites.

4. Conclusion

Changes in hydrogen dilution resulted in the production of very ordered hydrogenated silicon thin films. A very good R^* value for Film A, deposited without hydrogen dilution, shows it to be a prime candidate for use as an intrinsic amorphous layer in a solar cell. It was also revealed that a high processing temperature leads to the deposition of a partially crystallized silicon film, without the addition of hydrogen to silane. No bonded hydrogen could be detected at this high substrate temperature and it is proposed that the hydrogen is trapped as H_2 molecules. Hydrogen dilution also induces crystallization of the network of Si atoms and it produces films similar to the best a-Si:H in terms of optical density and absorption. The sample prepared at high

hydrogen dilution was shown to contain proto-crystalline material that induced a low energy band gap. Lastly, XRD analysis failed to detect very small crystallites in the films on glass whereas Raman spectroscopy revealed the most interesting features.

Acknowledgements

This work was supported by the NRF of South Africa (GUN 2050646). The authors also wish to thank Utrecht University for the Raman spectroscopy measurements.

References

- [1] Q. Wang, G. Yue, J. Li, D. Han, *Solid State Commun.* 113 (2000) 175.
- [2] D. Peiró, J. Bertomeu, C. Voz, M. Fonrodona, D. Soler, J. Andreu, *Mater. Sci. Eng., B* 69–70 (2000) 563.
- [3] A.H. Mahan, J. Carapella, B.P. Nelson, M. Vanecek, I. Balberg, *J. Appl. Phys.* 69 (1991) 6728.
- [4] P. Brogueira, J.P. Conde, S. Arekat, V. Chu, *J. Appl. Phys.* 79 (1996) 8748.
- [5] J. Doyle, R. Robertson, G.H. Lin, M.Z. He, A. Gallagher, *J. Appl. Phys.* 64 (1988) 3215.
- [6] D.L. Staebler, C.R. Wronski, *Appl. Phys. Lett.* 31 (1977) 292.
- [7] H. Matsumura, *Jpn. J. Appl. Phys.* 30 (1991) L1522.
- [8] M. Heintze, R. Zedlitz, H.N. Wanka, M. Schubert, *J. Appl. Phys.* 79 (5) (1996) 2699.
- [9] R. Swanepoel, *J. Phys. E: Sci. Instrum.* 16 (1983) 1214.
- [10] J. Daey Ouwens, R.E.I. Schropp, *Mater. Res. Soc. Symp. Proc.* 297 (1995) 27.
- [11] A.J.M. Berntsen, PhD thesis, Utrecht University, Utrecht, The Netherlands, 1993.
- [12] E. Bustarret, M.A. Hachicha, M. Brunel, *Appl. Phys. Lett.* 52 (1988) 1675.
- [13] R.A. Street, *Hydrogenated Amorphous Silicon*, Cambridge University Press, 1991, p. 2.
- [14] R.E. Norberg, D.J. Leopold, P.A. Fedders, *J. Non-Cryst. Solids* 227–230 (1998) 124.
- [15] R. Borzi, P.A. Fedders, P.H. Chan, J. Herberg, D.J. Leopold, R.E. Norberg, *J. Non-Cryst. Solids* 299–302 (2002) 205.
- [16] D. Beeman, R. Tsu, M.F. Thorpe, *Phys. Rev., B* 32 (1985) 874.
- [17] A.H. Mahan, J. Yang, S. Guha, D.L. Williamson, *Mater. Res. Soc. Symp. Proc.* 557 (1999) 269.